Liquid Crystals
Publication details, including instructions for authors and subscription information:
http://www.informaworld.com/smpp/title~content=t713926090

Synthesis and ferroelectric properties of chiral swallow-tailed liquid crystals derived from (L)-lactic acid

S. -L. Wu[a]; C. -Y. Lin[a]
[a] Department of Chemical Engineering, Tatung University, 40 Chungshan N. Rd., 3rd Sec., Taipei 104, Taiwan, ROC,

Online publication date: 11 November 2010

To cite this Article Wu, S. -L. and Lin, C. -Y.(2003) 'Synthesis and ferroelectric properties of chiral swallow-tailed liquid crystals derived from (L)-lactic acid', Liquid Crystals, 30: 4, 471 — 477
To link to this Article: DOI: 10.1080/0267829031000089898
URL: http://dx.doi.org/10.1080/0267829031000089898

LIQUID CRYSTALS, 2003, VOL. 30, NO. 4, 471–477

Taylor & Francis
Taylor & Francis Group

Synthesis and ferroelectric properties of chiral swallow-tailed liquid crystals derived from (L)-lactic acid

S.-L. WU* and C.-Y. LIN

Department of Chemical Engineering, Tatung University, 40 Chungshan N. Rd., 3rd Sec., Taipei 104, Taiwan, ROC

(*Received 12 August 2002; accepted 11 December 2002*)

Three homologous series of chiral swallow-tailed materials derived from (L)-lactic acid were prepared. Structural effects on the mesomorphic and physical properties were investigated in terms of (i) the variation of non-chiral peripheral length chain, (ii) the variation of swallow-tailed groups and straight alkyl chain at the chiral tails, and (iii) lateral halogen substituents in the core of the molecules. The mesophases and their corresponding transition temperatures were identified by optical polarized microscopy and differential scanning calorimetry. The physical properties of the ferroelectric SmC* phases such as switching current, spontaneous polarization and electro-optical response were also measured and compared.

1. Introduction

Achiral materials with swallow-tailed moieties have been demonstrated to possess the SmC_{alt} phase with antiferroelectric-like structure [1, 2]. The chiral swallow-tailed material (*S*)-EP10PBNP, derived from optically active (2*S*)-2-(6-hydroxy-2-naphyl)propionic acid, with 2-ethylpropanol as a swallow-tailed group, has been proved to possess antiferroelectricity [3].

Thus, in this work we designed three new series of chiral swallow-tailed materials derived from optical active (L)-lactic acid, with appropriate alkanols as chiral swallow-tailed groups, for the investigation of structure–property relationships. The three homologous series of chiral compounds, whose general structural formulae are depicted below, are (i) 1-ethylpropyl (*S*)-2-[4-(4′-alkyloxybiphenylcarbonyloxy)phenylcarbonyloxy]propionates, I(*m*,2,2), (ii) 1-alkylalkyl and 1-propyl (*S*)-2-[4-(4′-decyloxybiphenylcarbonyloxy)phenylcarbonyloxy]propionates, II(*m*,*n*,*q*), and (iii) laterally halogenated 1-ethylpropyl (*S*)-2-[4-(4′-decyloxybiphenylcarbonyloxy)benzoyloxy]propionates, III(*X*,*Y*). It is noted that (L)-lactic acid is a commercially available chiral compound and has been widely used as a chiral moiety for the preparation of chiral liquid crystals [4–9].

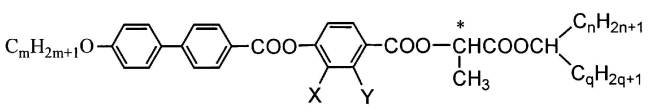

I(m, n, q; m=8~12, n=q=2, X=Y=H)
II(m, n, q; m=10, n=0, 2, 3, 4, q=2, 3, 4, X=Y=H)
III(X, Y; X=F, Cl, Y=F, Cl, m=10, n=q=2)

*Author for correspondence; e-mail: slwu@ttu.edu.tw

2. Experimental

2.1. *Characterization of the materials*

The chemical structures for intermediates and target materials were analysed by nuclear magnetic resonance spectroscopy using a Jeol EX-400 FTNMR spectrometer. Purity was checked by thin layer chromatography and further confirmed by elemental analysis using a Perkin-Elmer 2400 spectrometer. Transition temperatures and phase transition enthalpies were determined by differential scanning calorimetry using a Perkin-Elmer DSC7 calorimeter at running rates from 1 to 20°C min^{-1}. Mesophases were principally identified by microscopic texture of the materials sandwiched between two glass plates by polarizing optical microscopy (POM) using a Nikon Microphot-FXA in conjunction with Instec HS1 hot stages.

The physical properties of ferroelectric phase for the materials were measured in anti-parallel aligned cells purchased from E.H.C. Co. Japan. The spontaneous polarization ($\mathbf{P}_S$) was measured by a triangular wave method [10]. The measurement of optical transmittance versus applied electric field was conducted using a He-Ne laser (5 mW, 632.8 nm) as a probe beam [11, 12]. The optical transmittance of the probe beam passing through the cell between crossed polarizers, whose axes were parallel and perpendicular to the smectic layer normal, was detected by a photodiode. The signals were detected with a HP54502A digital oscilloscope. The voltage applied to the cell was produced by an arbitrary waveform generator (AG1200) and amplified by a homemade power preamplifier.

Liquid Crystals ISSN 0267-8292 print/ISSN 1366-5855 online © 2003 Taylor & Francis Ltd
http://www.tandf.co.uk/journals
DOI: 10.1080/0267829031000089898

2.2. *Preparation of materials*

The chiral starting material, (L)-lactic acid, was purchased from Fluka Co. Chem., Japan, with purity greater than 99%. Thin layer chromatography was performed with TLC sheets coated with silica; spots were detected by UV irradiation. Silica gel (MN kieselgel 60, 70–230 mesh) was used for column chromatography. The organic solvents dichloromethane (CH_2Cl_2) and tetrahydrofuran (THF), were purified by treatment with CaH_2 and $LiAlH_4$, respectively, and distilled before use.

The synthetic procedures for the target compounds were carried out as outlined in the scheme. Detailed procedures for the syntheses of compounds I(*m*,2,2), as examples, are described below. Elemental analysis data are given in table 1.

2.2.1. *4-(4-Alkyloxyphenyl)benzoic acids, **1**(m = 8–12)*

4-(4-Hydroxyphenyl)benzoic acid (25 mmol) and ethanol (200 ml) were mixed; a solution of potassium hydroxide (50 mmol), potassium iodide (KI) (3.6 mmol) and distilled water (50 ml) was then added, and the mixture heated under reflux for 1 h. 1-Bromoalkane (75 mmol) was then added dropwise and reflux continued for a further 12 h. Aqueous potassium hydroxide (KOH) (100 ml, 10%) was added and the reflux continued for 2 h. After cooling to the room temperature, the mixture

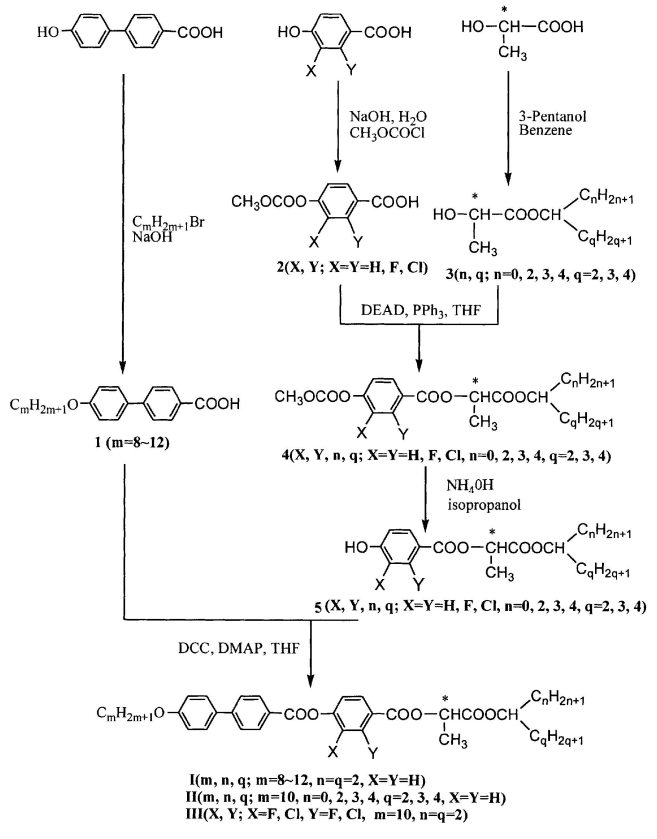

Scheme.

Table 1. The results of elemental analysis for the target compounds.

	Theoretical		Experimental	
Compounds	%C	%H	%C	%H
I(8,2,2)	73.46	7.48	73.30	7.48
I(9,2,2)	73.75	7.46	73.74	7.71
I(10,2,2)	74.02	7.79	73.86	7.85
I(11,2,2)	74.28	7.93	74.03	7.88
I(12,2,2)	74.53	8.07	74.35	8.12
II(10,0,2)	73.44	7.53	74.24	7.52
II(10,3,3)	74.50	8.13	74.50	8.20
II(10,4,4)	74.97	8.39	74.83	8.36
III(H,F)	71.90	7.46	71.89	7.51
III(F,H)	71.90	7.46	71.83	7.50
III(H,Cl)	70.08	7.27	70.09	7.27
III(Cl,H)	70.08	7.27	70.04	7.27

was acidified with 5% HCl and filtered. The crude product was washed with cold water and recrystallized from glacial acetic acid and absolute ethanol; 60–70% yields of compounds **1**(*m* = 8–12) were obtained.

2.2.2. *4-Methoxycarbonyloxybenzoic acid, **2**(H,H)* [13]

To a solution of sodium hydroxide (175 mmol) in water (200 ml) maintained at 0°C, 4-hydroxybenzoic acid (65 mmol) was added with vigorous stirring. Methyl chloroformate (105 mmol) was then added slowly to the resulting suspension which was maintained at 0–5°C. The resulting slurry was stirred for a further 4 h and brought to pH = 5 by the addition of conc. HCl and water (1 : 1). The voluminous precipitate was filtered off and recrystallized from ethanol to give a white solid; 85% yield of compound **2**(H,H) was obtained. ^{1}H NMR (400 MHz, $CDCl_3$): δ (ppm) 8.15 (s, 1H, $-COO\underline{H}$), 8.10–7.23 (d, d, 4H, $-Ar\underline{H}$), 3.92 (s, 3H, $-OC\underline{H}_3$).

2.2.3. *1-Ethylpropyl (S)-2-hydroxypropionate, **3**(2,2)* [9]

(*S*)-2-Hydroxypropionic acid (130 mmol) and 3-propanol (150 mmol) in dry benzene (30 ml) was heated under reflux with a Dean and Stark trap for 10 h. Benzene was evaporated and the residue distilled *in vacuo*; a 45% yield of 1-ethylpropyl (*S*)-hydroxypropionate, **3**(2,2) was collected as colourless liquid. ^{1}H NMR (400 MHz, $CDCl_3$): δ (ppm) 0.84–0.76 (m, 6H, $-(CH_2C\underline{H}_3)_2$), 1.36–1.31 (d, 3H, $-CHC\underline{H}_3$), 1.55–1.38 (m, 4H, $-CH(C\underline{H}_2CH_3)_2$), 3.84 (s, 1H, $-O\underline{H}$), 4.21–4.15 (m, 1H, $-COOC\underline{H}-$), 4.76–4.70 (m, 1H, $-COOC\underline{H}(CH_2-)_2$.

2.2.4. *1-Ethylpropyl (S)-2-[4-(methoxycarbonyloxy)-phenoyloxy]propionate, **4**(H,H,2,2)* [14]

A solution of diethyl azodicarboxylate (DEAD, 13 mmol) and compound **2**(H,H) (13 mmol) in anhydrous THF (10 ml) was added dropwise to a solution of

triphenylphosphine (Ph_3P, 13 mmol) and compound **3**(2,2) (10 mmol) in anhydrous THF (10 ml) at room temperature with vigorous stirring; the reaction soon started. After standing overnight at room temperature, triphenylphosphine oxide was removed by filtration and the THF was removed under vacuum. After the work-up procedure, the product was isolated by column chromatography over silica gel (70–230 mesh) using ethyl acetate/hexane (v/v = 2/8) as eluent to give a colourless liquid; 75% yield of compound **4**(H,H,2,2) was obtained. ^{1}H NMR (400 MHz, $CDCl_3$): δ (ppm) 0.91–0.82 (m, 6H, $-(CH_2C\underline{H}_3)_2$), 1.56–1.49 (d, 3H, $-CHC\underline{H}_3$), 1.62–1.58 (m, 4H, $-CH(C\underline{H}_2CH_3)_2$), 3.90 (s, 3H, $-COOC\underline{H}_3$), 4.84–4.80 (q, 1H, $-COOC\underline{H}(CH_2)_2-$), 5.30–5.27 (m, 1H, $-COOC\underline{H}CH_3-$, $-Ar\underline{H}$), 8.12–7.23 (d, d, 4H).

2.2.5. *1-Ethylpropyl (S)-2-(4-hydroxyphenylcarbonyloxy)-propanoate,* ***5****(H,H,2,2)* [14]

Compound **4**(H,H,2,2) (3 mmol) were stirred in a mixture of isopropanol (90 ml) and ammonia (28%, 30 ml) at room temperature for 50 min (TLC analysis revealed a complete reaction) and then poured into water (40 ml) with stirring. The product was extracted with dichloromethane (3 × 50 ml). The combined organic extracts were washed with brine (3 × 50 ml), dried ($MgSO_4$), filtered and evaporated to give a colourless oil. The oil was purified by flash column chromatography over silica gel (70–230 mesh) using dichloromethane as eluent. The solated product was then dried *in vacuo*; 80% yield of compound **5**(H,H,2,2) was obtained. ^{1}H NMR (400 MHz, $CDCl_3$): δ (ppm) 0.87–0.79 (m, 6H, $-(CH_2C\underline{H}_3)_2$), 1.58–1.46 (d, 3H, $-CHC\underline{H}_3$), 1.76–1.58 (m, 4H, $-CH(C\underline{H}_2CH_3)_2$), 4.81–4.75 (m, 1H, $-COOC\underline{H}(CH_2)$), 5.23–5.18 (q, 1H, $-COOC\underline{H}CH_3-$), 6.27 (s, 1H, $-O\underline{H}-$), 7.85–6.73 (d, d, 4H, $-Ar\underline{H}$).

2.2.6. *1-Ethylpropyl (S)-2-[4-(4′-alkyloxybiphenyl-carbonyloxy)phenylcarbonyloxy]propanoates, I(m,2,2; m = 8–12)* [14]

A mixture of a 4-(4′-alkyloxyphenyl)benzoic acid (2.8 mmol), compound **5** (0.8 g, 3.1 mmol), *N*,*N*′-dicyclohexylcarbodiimide (2.8 mmol), 4-dimethylaminopyridine (0.28 mmol) and dry THF (15 ml) was stirred at room temperature for three days. The precipitate was filtered off and the filtrate washed with 5% acetic acid solution (3 × 50 ml), 5% saturated aqueous sodium hydrogen carbonate (3 × 50 ml) and water (3 × 50 ml); the filtrate was then dried over anhydrous magnesium sulfate ($MgSO_4$) and concentrated in vacuum. The residue was purified by column chromatography over silica gel (70–230 mesh) using dichloromethane as eluent. Recrystallization from absolute ethanol 40% yield of final products were obtained. The chemical shifts for compound I(10,2,2), as an example, in ^{1}H NMR (400 MHz, $CDCl_3$) are: δ (ppm) 1.81–0.84 (m, 32H, $RC\underline{H}_2C\underline{H}_3$), 4.01–3.98 (t, 2H, $ArOC\underline{H}_2$), 4.86–4.80 (m, 1H, $-COOC\underline{H}$), 5.33–5.27 (q, 1H, $-COOC\underline{H}CH_3COO$), 8.22–6.98 (d, d, 12H, $-Ar\underline{H}$).

2.2.7. *Syntheses of compounds II(10,n,q) and III(X,Y)*

These two series of final products were synthesized by the same procedures as described above.

3. Results and discussion

3.1. *Mesomorphic properties*

The SmA* phase was characterized by the formation of focal-conic texture and the SmC* phase by the formation of broken focal-conic texture. All compounds displayed enantiotropic SmA* and SmC* phases, while compound II(10,0,2) possessed an additional unidentified SmX* phase. The mesophases and their transition temperatures, measured by DSC, for the target compounds are shown in table 2.

A plot of phase transition temperature versus elongated alkyl chain length *m* for the compounds I(*m*,2,2) is shown in figure 1. This series of compounds exhibit a wide temperature range for the ferroelectric SmC* phase. As shown by this figure, the clearing point decreases as

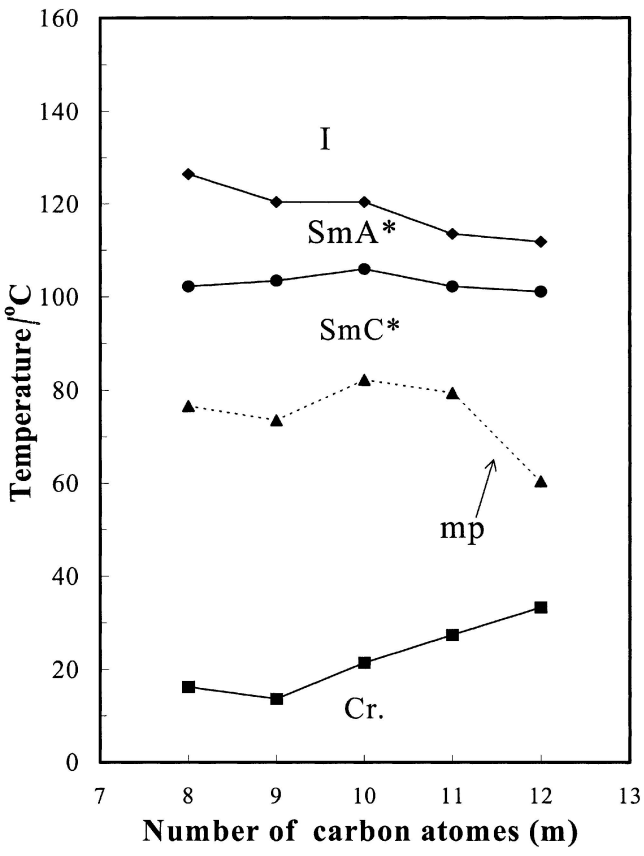

Figure 1. A plot of transition temperature as a function of terminal alkyl chain length for compounds I(*m*,2,2) on cooling.

Table 2. The transition temperatures (°C) and associated enthalpy data (J g^{-1}, in parentheses) for chiral materials.

	Transition temperatures[a]											
Compound	I		SmA*		SmC*		SmX*			Cr	m.p.	
I(8,2,2)	•	126.4 (4.26)	•	102.2 (0.25)	•	16.2 (6.42)				•	76.6 (27.98)	
I(9,2,2)	•	120.4 (2.42)	•	103.4 (0.35)	•	13.5 (6.59)				•	73.5 (22.37)	
I(10,2,2)	•	120.4 (3.45)	•	105.9 (0.63)	•	21.4 (13.58)				•	82.2 (34.76)	
I(11,2,2)	•	113.5 (4.74)	•	102.2 (2.23)	•	27.4 (29.27)				•	79.4 (46.02)	
I(12,2,2)	•	111.6 (2.55)	•	100.9 (0.92)	•	31.3 (29.96)				•	60.43 (43.72)	
II(10,0,2)	•	146.5 (5.59)	•	117.8 (0.54)	•	31.6 (4.09)	•	16.83 (19.4)		•	60.3 (45.81)	
II(10,3,3)	•	101.3 (9.49)	•	85.5 (2.67)	•	21.5 (18.04)				•	38.7 (32.04)	
II(10,4,4)	•	89.6 (1.05)	•	69.7 (0.51)	•	20.5 (17.10)				•	48.7 (36.95)	
III(F,H)	•	95.0 (6.45)	•	74.5 (0.54)	•	20.4 (29.37)				•	38.8 (35.74)	
III(Cl,H)	•	73.2 (4.26)	•	45.5 (0.01)	•	−1.9 (12.13)				•	34.7 (20.22)	
III(H,F)	•	113.1 (6.78)	•	95.6 (0.36)	•	14.3 (19.01)				•	27.4 (24.94)	
III(H,Cl)	•	86.1 (3.99)	•	69.6 (0.53)	•	10.8 (4.44)				•	34.7 (20.22)	

[a] Recorded by DSC thermograms at cooling rates of 5°C min^{-1}.

the series is ascended, but the SmC*–Cr transition temperature is increased. That is, the thermal stabilities of the SmA* and SmC* phases are suppressed as *m* is increased.

A phase diagram as a function of straight alkyl chain and swallow-tailed groups at the chiral tail for compounds I(10,2,2) and II(10,*n*,*q*), respectively, on cooling is plotted in figure 2. It can be seen that the compound with a straight alkyl chain at the chiral tail has higher thermal stability of the SmA* and SmC* phases. This behaviour provides evidence that an increase in size of chiral tail may play an important role in suppressing smectic phases. Figure 2 also shows that the clearing point and SmA*–SmC* transition temperature decrease as the length of swallow-tailed alkyl chain increases. The extending swallow-tailed alkyl chain length stabilizes the SmA* phase but suppresses SmC* phase formation.

A phase diagram as a function of lateral halogen substitution in the core of compounds III(*X*,*Y*) is plotted in figure 3. It is seen that the compounds with lateral halogen substituents in the core of the molecules suppress the formation of mesophases and decrease transition temperatures and melting point. This is because, in the

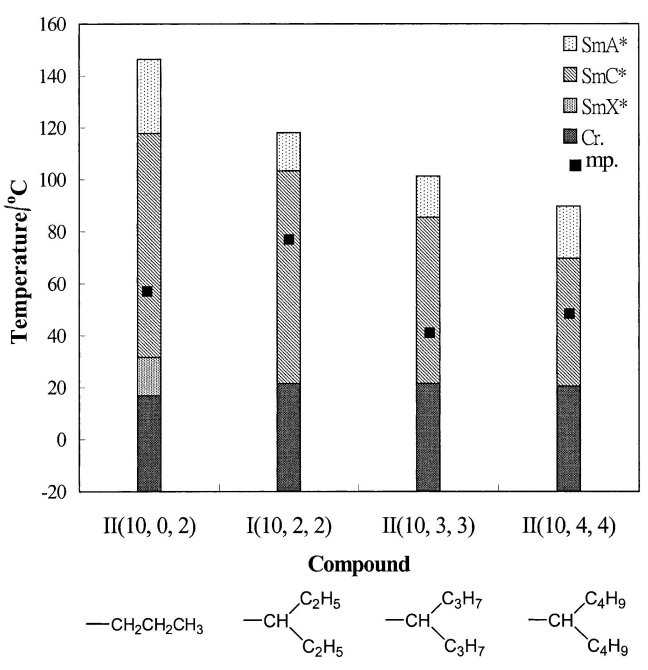

Figure 2. A plot of transition temperature as a function of straight alkyl chain and swallow-tailed groups for compounds II(10,*n*,*q*) on cooling.

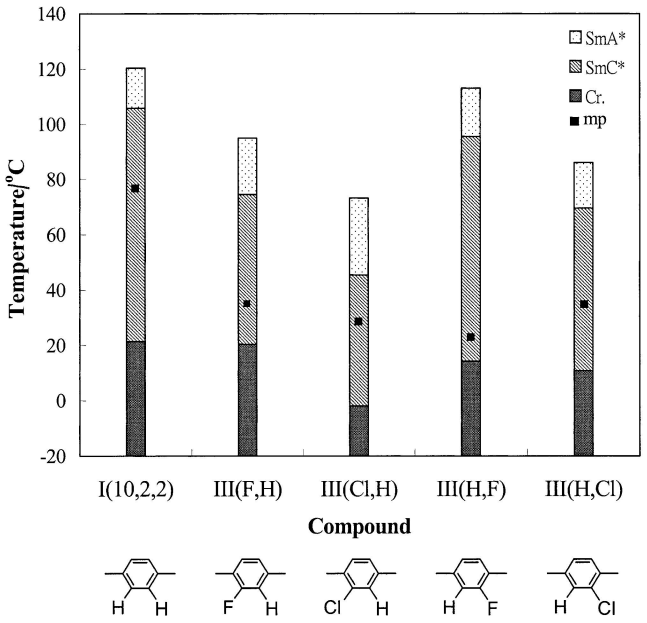

Figure 3. A plot of transition temperature as a function of halogen substituents in the core of compounds III(X,Y) on cooling.

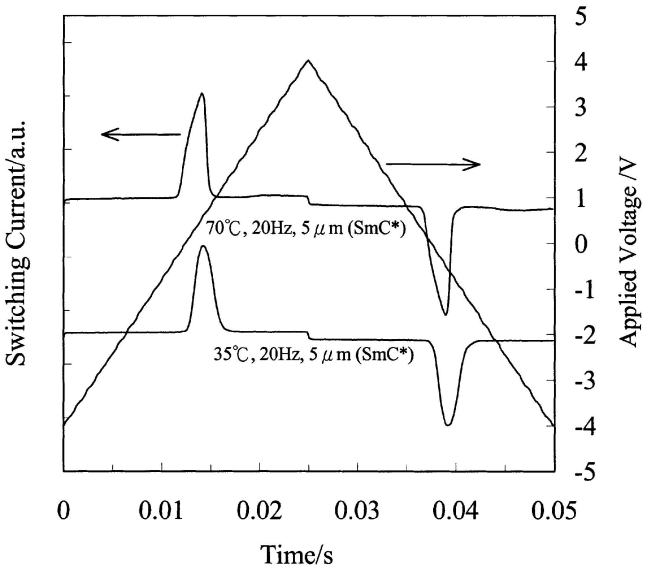

Figure 4. Switching behaviour of I(10,2,2) in the SmC* phase at 70 and 35°C.

case of a fluoro substituent, although the size of fluoro substituent is small (1.47 Å), it is still slightly larger than hydrogen (1.20 Å). Thus a lateral fluoro substituent exerts a steric effect. Moreover, the fluoro substituent has higher polarity (the highest electronegativity known, 4.0). This unique combination of steric and polarity effects causes significant disruption to the liquid crystal phase stability. Comparing III(F,H) with III(H,F), the material with 2-fluoro substitution has a higher transition temperature than that with 3-fluoro substitution, suggesting that the 2-fluoro substituent is sterically shielded, and molecular broadening minimized [15]. The size of a chloro substituent (1.75 Å) is much larger than that of hydrogen, thus, in comparing the chloro-substituted compound III(Cl,H) to the non-substituted compound I(10,2,2), the former has a much lower transition temperature than the latter. It can be clearly seen from figure 3, that the largest size of the chloro substituent greatly affects the formation of mesophases.

3.2. *Switching behaviour*

The physical properties of the compounds were measured in 5 μm homogeneous cells. Figure 4 shows the electrical switching response of I(10,2,2) under a triangular wave voltage with field frequency 20 Hz and amplitude 8 $V_{p\text{-}p}$. The switching currents display one current peak from 102 to 35°C similar to the behaviour reported for the SmC* phase [16].

3.3. *Spontaneous polarization (P_s)*

The temperature dependence of the spontaneous polarization ($\mathbf{P}_S$) of the target compounds was measured and is illustrated in figures 5–7. Figure 5 shows that the maximum $\mathbf{P}_S$ values of compounds I(m,2,2) are in the range of 107–119 nC cm^{-2}. No signification correlation of $\mathbf{P}_S$ values with variation of alkyl chain length was found.

Figure 6 shows the $\mathbf{P}_S$ of compounds II(10,n,q). The maximum $\mathbf{P}_S$ values are in a range of 97–119 nC cm^{-2}. Comparing II(10,0,2) with I(10,2,2), the chiral compound containing the straight alkyl chain has a lower spontaneous polarization. It seems that the dipole moment originating in the chiral compounds containing the swallow-tailed chain enhances spontaneous polarization.

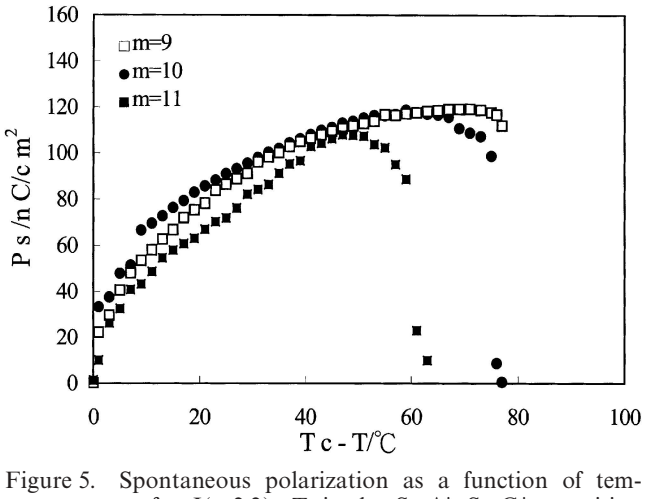

Figure 5. Spontaneous polarization as a function of temperature for I(m,2,2). T_c is the SmA*–SmC* transition temperature.

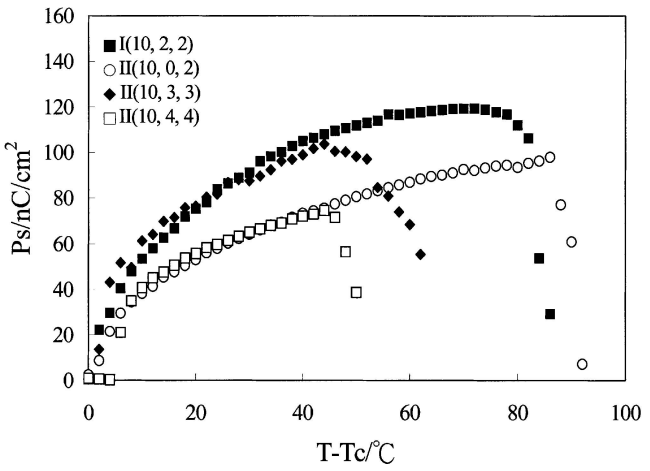

Figure 6. Spontaneous polarization as a function of temperature for II(10,*n*,*q*). T_c is the SmA*–SmC* transition temperature.

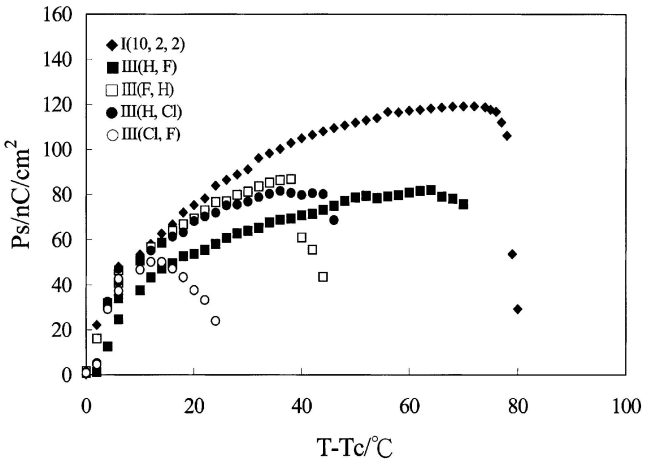

Figure 7. Spontaneous polarization as a function of temperature for compounds I(10,2,2) and III(*X*,*Y*). T_c is the SmA*–SmC* transition temperature.

Comparing I(10,2,2) with II(10,3,3), the compound with the 1-ethylpropyl group has higher $\mathbf{P}_S$ values then that with the 1-propylbutyl group. This result suggests that extending the swallow-tailed chain length depresses the $\mathbf{P}_S$. This phenomenon is presumably due to the increasing swallow-tailed length resulting in increasing mass at the chiral tail, thus reducing the polarization.

Figure 7 shows $\mathbf{P}_S$ values of compounds III(*X*,*Y*), with the non-substituted compound I(10,2,2) for comparison. I(10,2,2) has higher $\mathbf{P}_S$ values than compounds III(*X*,*Y*), due to the compensating effect of the lateral halogen substituents with respect to the $\mathbf{P}_S$. That is, the halogen substituent points away from the direction of the chiral methyl group, hence diminishing the observed $\mathbf{P}_S$ [17].

3.4. *The electro-optical responses*

The electro-optical responses were obtained under crossed polarizers where the axes of polarizer and analyser were parallel and perpendicular, respectively, to the smectic layer normal in a homogeneously aligned cell. Figure 8 illustrates the responses of transmittance versus electric field on application of a field of triangular waveform for the representative compounds I(10,2,2), II(10,0,2) and III(Cl,H) in a 5 μm homogeneous cell. The responses are critically dependent on temperature and frequency. As the temperature decreases, the maximum transmittance values increase, presumably due to an increase in tilt angle. The optical switching of II(10,0,2) in the SmC* phase showed typical ferroelectric normal hysteresis loops at 0.5 Hz of applied frequency. However, the optical switching for chiral swallow-tailed compounds, for example I(10,2,2), displayed U-shaped switching at certain temperatures and 0.5 Hz of applied frequency in the SmC* phase. It seems that hysteresis-free switching is easier to generate in the chiral compounds containing the swallow-tailed group than in compounds with

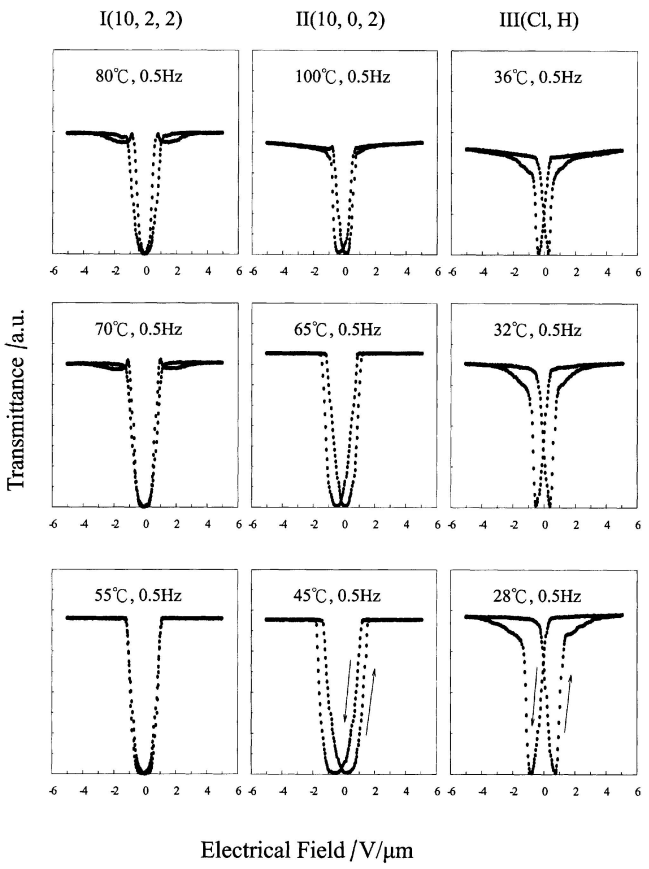

Figure 8. Electro-optical responses of transmittance versus electric field obtained from compounds I(10,2,2), II(10,0,2) and III(Cl,H) in the SmC* phase at various temperatures and frequencies of applied triangular wave.

a straight alkyl chain. It can be concluded that hysteresis-free U-shaped switching behaviour is affected not only by temperature and applied frequency in the smectic SmC* phase, but also by the structure of the chiral tail groups of the molecules. It is also interesting to find that the electro-optical response in compound III(Cl,H) at 0.5 Hz displays a W-shaped feature in the SmC* phase. This W-shaped switching behaviour in the SmC* phase will be further investigated and reported elsewhere in the future.

4. Conclusion

Three series of chiral swallow-tailed compounds derived from (L)-lactic acid have been demonstrated to possess the ferroelectric SmC* phase. The relationship between molecular structure and physical properties in the SmC* phase has been primarily established. The high magnitudes of $\mathbf{P}_S$ and wide temperature range of the SmC* phase in some ferroelectric liquid crystals may be useful in mixtures for liquid crystal device application.

The authors are grateful to the National Science Council of the Republic of China (NSC 90-2216-E-036-010 and 91-2216-E-036-003).

References

[1] Booth, C. J., Dunmur, D. A., Goodby, J. W., Haley, J., and Toyen, K. J., 1996, *Liq. Cryst.*, **20,** 387.
[2] Wu, S.-L., and Chiang, C.-T., 2002, *Liq. Cryst.*, **29,** 39.
[3] Wu, S.-L., and Hsieh, W.-J., 1999, *J. mater. Chem.*, **11,** 852.
[4] Kašpar, M., Glogarová, M., Hamplová, V., Sverenyák, H., and Pakhomov, S. A., 1993, *Ferroelectrics*, **148,** 103.
[5] Kašpar, M., Sverenyák, H., Hamplová, V., Glogarová, M., Pakhomov, S. A., Vanek, P., and Trunda, B., 1995, *Liq. Cryst.*, **19,** 775.
[6] Kašpar, M., Hamplová, V., Pakhomov, S. A., Stibor, I., Sverenyák, H., Bubnov, M. A., Glogarová, M., and Vanek, P., 1997, *Liq. Cryst.*, **22,** 557.
[7] Hamplová, V., Kašpar, M., Pakhomov, S., Bubnov, A., and Glogarová, M., 1999, *Mol. Cryst. liq. Cryst.*, **322,** 181.
[8] Buvnov, A., Hamplová, V., Kašpar, M., Vanek, P., Pociecha, D., and Glogarová, M., 2001, *Mol. Cryst. liq. Cryst.*, **366,** 547.
[9] Kašpar, M., Hamplová, V., Novotná, V., Glogarová, M., Pociecha, D., and Vanek, P., 2001, *Liq. Cryst.*, **28,** 1203.
[10] Miyasato, K., Abe, S., Takezoe, H., Fukuda, A., and Kuze, E., 1983, *Jpn. J. appl. Phys.*, **22,** L661.
[11] Chandani, A. D. L., Hagiwara, T., Suzuki, Y., Ouchi, Y., Yakazoe, H., and Fukuda, A., 1988, *Jpn. J. appl. Phys.*, **27,** L729.
[12] Lee, J., Chandani, A. D., Itoh, K., Ouchi, Y., Takezoe, H., and Fukuda, A., 1990, *Jpn. J. appl. Phys.*, **29,** 1122.
[13] Chin, E., and Goodby, J. W., 1986, *Mol. Cryst. liq. Cryst.*, **141,** 311.
[14] Booth, G. J., Dunnur, D. A., Goodby, J. W., and Toyne, K. J., 1996, *Liq. Cryst.*, **28,** 815.
[15] Colling, P. J., and Hird, M., 1998, *Introduction to Liquid Crystals Chemistry and Physics*, p. 70.
[16] Fukuda, A., Takanishi, Y., Isozaki, T., Ishikawa, K., and Takezoe, H., 1994, *J. mater. Chem.*, **4,** 997.
[17] Parghi, D. D., Kelly, S. M., and Goodby, J. W., 1999, *Mol. Cryst. liq. Cryst.*, **332,** 313.